A steady-state analysis of distribution networks by diffusion-limited-aggregation and multifractal geometry

Nicolas Retière, Yousra Sidqi, Pierre Frankhauser

A steady-state analysis of distribution networks by diffusion-limited-aggregation and multifractal geometry

N. Retière[a,*], Y. Sidqi[b], P. Frankhauser[c]

[a] *Univ. Grenoble Alpes, CNRS, Grenoble INP[1] , G2elab, France*
[b] *Lucerne University of Applied Sciences and Arts, Engineering and architecture, Switzerland*
[c] *Université Bourgogne Franche-Comté, CNRS, Thema, France*

Abstract

Global energy transformation, urban growth and the increasing share of electricity in energy consumption stimulate the development of electrical distribution systems. In most cases, the structure of distribution networks has been the result of progressive decisions limited by technical, socio-economic and spatial constraints. These decisions are taken with the help of dedicated tools that fail in grasping in a simple way the connections between the structural choices and the achieved performances. To improve planning process, a new approach is proposed which is based on multifractality to connect the distribution system's network structure and steady-state properties. The structure of distribution grids is modeled by coupling a Diffusion-Limited-Aggregation approach and a binomial multiplicative process. The multifractal spectrum of the synthesized grids is calculated from a power flow and shows how the structural parameters are linked to the steady-state values (voltages and losses). The results are compared to realistic test cases. The article finally concludes on the interest of multifractality to grade distribution grids and the advantages of fractal architectures for future power networks.

Keywords: Distribution networks, Power flow, Voltage, Losses, Fractal geometry, Graph theory, Principal component analysis

1. Introduction

Power networks are central for electricity distribution. 97 % of the world population lives at less than 10 km of a medium power line [1]. In Europe, the distribution lines lenght is 13 times the distance to Moon and back. According to IEA world energy investment report 2020, the annual investment in distribution

*Corresponding author
Email addresses: nicolas.retiere@univ-grenoble-alpes.fr (N. Retière), yousra.sidqi@hslu.ch (Y. Sidqi), pierre.frankhauser@univ-fcomte.fr (P. Frankhauser)
[1] Institute of Engineering Univ. Grenoble Alpes

networks is around USD 200 billions and represents two-thirds of the global investment in power networks. The share of the distribution network cost in the household customer bill is already around 30 % in European countries [2]. This pivotal role of distribution networks is increasing with the transformation of the energy system to reduce the greenhouse gas emission and the massive integration of renewable, storage and smart technologies. The planning and operation of distribution networks should be rethought to cope with the new challenges related to this profound change of the energy system.

Limited investment capabilities, low operation cost, power quality, reliability are challenges which were already addressed by planning and operation of distribution networks. But with the increasing share of dispersed renewable energy sources, the planners and operators face new issues [3, 4]. The consumers become prosumers, providing energy to the electrical system, and local energy communities emerge where members take collective actions, e.g. distributed generation. Hence, electrical distribution networks must evolve to cope with the bidirectionnal flows of powers. Extreme events or conflicts also brought the attention to resiliency and how to take advantage of decentralization of energy sources and microgrids to ensure resilient operation of distribution networks [5, 6].

The electrical properties of distribution grids and how they enable flow of energy with low voltage drops, reduced losses and high reliabiliy, arise from their structure. In most cases, the shape of distribution networks has been the result of progressive decisions limited by technical, socio-economic and spatial constraints [7, 8]. The decisions are taken with the help of dedicated tools that are specialized in detailed representation of power systems for simulation and optimization [9, 10]. These tools fail in grasping in a simple way the connections between the structural choices and the achieved performances. Our main goal is thus to provide a method to understand how the distribution system's electrical properties emerge from the way the distribution networks are shaped [11]. In this paper, we propose a two-point approach. A Diffusion-Limited-Aggregation technique is used to model how distribution networks' structures are shaped. A multifractal formalism is adopted to characterize the links between the shaped structures and the steady-state properties of the networks.

Fractality is a well-known approach used for natural or artificial complex systems. It is intended to study the global features of their geometrical arrangement without paying much attention to the detailed description of the structure [12]. It allows investigating a system across scales unlike other approaches which focus on particular scales. In 1985, Frisch and Parisi proposed a generalization of fractality. They qualify of "multifractal" the distribution of singularities in turbulence [13]. Since then, multifractality has been applied in numerous fields, especially for investigating urban forms and networks [14, 15]. In this paper, the multifractal formalism is proposed to characterize the singularities in the nodal voltage profiles of distribution networks.

There are few realistic and available data to perform extensive investigations of the links between the structure of networks and their performances. Most of the open-source data are often aggregated values on generation and loads and

the diversity of available structural data for distribution power grids is limited. Therefore, this paper proposes an original approach to model in a very simple way the network topology and generate synthetic but realistic distribution grids. It is inspired by Diffusion-Limited Aggregation approach (DLA). DLA is used to study growth phenomena of random structures [16]. It has already been adopted to model growth of urban fabrics [17]. Electrical distribution networks topologies depend on the space distribution of buildings and streets map. Therefore, DLA may also be a good candidate to mimic networks structure. Another motivation is the apparent self-similarity in the branching process of distribution grids as observed in DLA clusters [16]. The growth modeling is completed by a binomial multiplicative cascade process to model the distribution of loads in the grid. The synthesized networks are multifractally and electrically characterized and the results are correlated with the DLA and binomial process parameters to link the structural and electrical properties of distribution power grids.

To the best of our knowledge, our paper brings two main contributions. It is the first-ever application of multifractal formalism to the steady-state analysis of electrical networks. The other very rare applications are about the classification of time signals [18, 19] or load forecasting [20]. Our DLA-inspired framework used to generate synthetic data is also an answer to a mathematical research priority for the future power grids listed by the National Academies of Sciences, Engineering, and Medicine [21].

The paper is organized as follows. In a first section, the multifractal analysis of the electrical variables in a distribution power grid is introduced. The paper focuses on the values of the nodal voltages that are crucial for a proper operation of the distribution grids. These values are obtained by a power flow calculation [22]. The second section shows a first application of the proposed multifractal formalism to a toy network built according to a binomial multiplicative cascade process. Theoretical results on the multifractal spectrum are available for this toy network and they are compared with the numerical values provided by our multifractal approach for validation purposes. Then, multifractal spectrum of three realistic distribution test networks are calculated and investigated. The data of the realistic cases are available in [23, 24, 25]. A fourth section is dedicated to the modeling and synthesis of realistic distribution networks by DLA and their multifractal analysis. A principal component analysis is performed to show the links between the structural parameters, the electrical performances and the multifractal spectrum. The last section concludes the paper by a discussion on the main achievements.

2. Multifractal spectrum of voltages

The power flows in network branches cause variations of node voltages. To ensure a high quality of power delivered to users and safe operation of connected devices, electrical installation shall comply standards that specify voltage ranges. Typical limits are $\pm 10\%$ around the nominal value. For verifying standard compliance, the magnitude of nodal voltages is computed by a power flow calculation [22].

A multiscale view of voltage values can be achieved by multifractality. Multifractals are a generalization of fractals when a single dimension cannot characterize the scaling behavior and a collection of generalized dimensions is used to describe the multifractal object and its scaling properties. The generalized dimensions are calculated from the q-th moments of the observed values on the investigated object.

The box counting method provides a way to compute these moments. The object is covered by boxes of size r and the number of elements in each non empty boxes is counted [26]. Moments can also be measured by correlation method, an easy-to-implement technique counting the number of points of the object located in a ball of radius r centered on the object.

Correlation methods were first introduced by Grassberger and Procaccia in 1983 to characterize attractors [27, 28, 29]. For a series x_i of observations, the correlation measure $C(r)$ is defined by [27, 30]:

$$C(r) = \lim_{n\to\infty} \frac{1}{n^2}\{\text{number of pairs}\,(x_i, x_j)\,\text{with}\,|x_i - x_j|\langle r\} \tag{1}$$

n is the number of observed points and r is the ball radius. In practice, the counting is done over a finite number N of observed points. It is repeated for various centers, the center is itself excluded from the counting and an average over the centers is finally done [26]. This method was generalized to higher order q of correlation integrals $C_q(r)$ to compute multifractal spectrum [31]:

$$C_q(r) = \left\{ \frac{1}{N} \sum_{i\in\mathcal{N}} \left[\frac{1}{N-1} \sum_{j\in\mathcal{N}\neq i} \Theta(r - |x_i - x_j|) \right]^{q-1} \right\}^{\frac{1}{q-1}} \tag{2}$$

$\mathcal{N}$ is the node set of size N. Θ is the Heaviside function.

The finite number of the observed points, the finite size, the borders of the studied object and the discretization of the measure are the main limitations of the correlation approach [26]. Most of these limitations are overcome by considering a large enough value of N and measuring the dimension over an adequate range between the smallest inter point gaps and the maximal radius of the object.

A straightforward adaptation of the correlation method for the measure of the multifractal spectrum of geometrical objects was proposed by Tel and Vicsek in 1989 [32]. It relies on the measure of the mass of the object within a ball of radius r centered on it. For an accurate determination, the measure is repeated and averaged over different centers, randomly distributed on the object. This method was in turn adapted to complex networks in 2005 and edge-weighted networks in 2015, respectively [33, 34]. The edge weights are used to measure the radius of the correlation ball. Inside each ball, the number of nodes is then counted. For multifractal characterization of networks, correlation measure is better adapted than box counting. The latter requires small box sizes to cover sparse areas of the network (e.g. termination lines) and that leads to an over exagerated total number of boxes to cover the whole grid [35]. Contrary to box

counting method, every correlation ball is centered on the network. So, there is no ball with too few points and the results are less sensitive to sparsity.

We propose a modified definition of the correlation measure for the characterization of nodal voltages in power networks. Our definition takes into account edges weights (line impedance values) and nodes weights (nodal voltage magnitudes). And to count the mass of the object, the weights are summed instead of the number of nodes. The definition of the q-th correlation measure expressed by equation (2) is then modified. It is now given by:

$$\langle \mu \rangle_q = \left\{ \frac{1}{N} \sum_{i \in \mathcal{N}} \omega_{v,i} \left[\mu_i(r) \right]^{q-1} \right\}^{\frac{1}{q-1}} \tag{3}$$

$\mathcal{N}$ is the node set of size N. $\omega_{v,i}$ is the weight of node i. It is equal to the nodal value normalized by the sum of all nodal values of the network. The measure μ_i is defined by the sum of the values $\omega_{v,j}$ of the nodes j located within a circle of radius r centered at the node i:

$$\mu_i(r) = \frac{1}{N-1} \sum_{j \in \mathcal{N} \neq i} \omega_{v,j} \Theta(r - d_{i,j}) \tag{4}$$

$d_{i,j}$ is related to the weighted distance between the nodes i and j. It is defined by the shortest path length between the nodes of the weighted graph. The edge weights of the graph are equal to the line impedance values. Θ is the Heaviside function.

The q-th generalized dimension is then given by [31]:

$$D_q = \lim_{r \to 0} \frac{\ln \langle \mu \rangle_q(r)}{\ln(r)} \tag{5}$$

The exponents q determine the resolution level. For large q, the high measured values are stressed whereas for low q small values are privileged.

Instead of computing the generalized dimensions, the Legendre transform (α, f) of $(q, (q-1)D_q)$ can be used to multifractally characterize an object. α gives the local regularity of the measures. According to the Hölder condition, the measures are locally singular in the points where $\alpha < 1$. Otherwise, they are locally constant. $f(\alpha)$ is the dimension of the set where are sitting the measures with the same singularity strenght α [36]. The number of boxes $n(r, \alpha)$ for which the measure scales with an exponent α is therefore such that $n(r, \alpha) \sim r^{-f(\alpha)}$. The determination of the singularity spectrum $f(\alpha)$ follows an approach inpired by [37] and is shown in Appendix A. Its implementation is straightforward and based on the power flow results and the distances between nodes of the network.

3. Singularity spectrum of a binomial electrical network

The multifractal spectrum of a toy network is first investigated to illustrate and validate our approach. The structure of the network is a path. It has

$N = 2^n + 1$ nodes. The line impedances are all equal to $\frac{1}{2^n}$. Every node i, except the source one s, is loaded. The load power value P_i result from a binomial multiplicative cascade such that:

$$P_i = p_{bin}^{k_i}(1 - p_{bin})^{n-k_i} \forall i \in \{0, 1, ..., 2^n - 1\} \tag{6}$$

k_i is the number of 0 in the binary fraction representation of $\frac{i}{n}$. If p is 0.5, all the loads are equal. If p is lower than 0.5, the loads are more concentrated at the termination nodes of the line, whereas for higher value than 0.5, the loads are situated closer to the source.

The source node balances the total load power and is given by:

$$P_s = -\sum_{i=0}^{2^n-1} P_i \tag{7}$$

This toy network has the same multifractal properties as the binomial multiplicative cascade. If the nodes with the same k_i are gathered into sets, for an infinite number of points, the fractal dimension of these sets can be theoretically determined and is given by [38]:

$$f(\xi) = -\frac{\xi \ln(\xi) + (1 - \xi) \ln(1 - \xi)}{\ln 2} \tag{8}$$

With: $\xi = \frac{k_i}{n}$.

The points belonging to the same set have an identical singularity strength expressed by:

$$\alpha(\xi) = -\frac{\xi \ln(p) + (1 - \xi) \ln(1 - p)}{\ln 2} \tag{9}$$

This theoretical spectrum $f(\alpha)$ is the multifractal spectrum of the distribution of the nodal load powers.

The theoretical spectrum of the nodal voltages is derived from a linear approximation of the power flow equations of the network. Let consider a network with N nodes. The non linear power flow equations are expressed by [22]:

$$I_i = \frac{P_i - jQ_i}{V_i^*} \tag{10}$$

I_i and V_i are the current and voltage at node $i \in \mathcal{N} = \{1, 2, ..., N\}$. P_i and Q_i are the nodal active and reactive power values respectively. They correspond to the power delivered by the generators or consumed by the loads connected at each node [22].

The node voltages are defined by:

$$V_i = |V_i| e^{j\phi_i} \tag{11}$$

The node currents are linked to the voltages by the bus admittance matrix Y such that:

$$I_i = \sum_{j=1}^{n} Y_{ij} V_j \tag{12}$$

The bus admittance matrix elements are given by:

$$Y_{ij} = G_{ij} + jB_{ij} \tag{13}$$

G_{ij}, respectively B_{ij} is the inverse value of the line resistance R_{ij}, respectively line reactance X_{ij}, between the nodes i and j. The value is zero if there is no line.

It comes:

$$\begin{aligned} P_i &= V_i \sum_{j=1}^{N} (G_{ij}|V_j|cos(\phi_{ij}) + B_{ij}|V_j|sin(\phi_{ij})) \\ Q_i &= V_i \sum_{j=1}^{N} (G_{ij}|V_j|sin(\phi_{ij}) - B_{ij}|V_j|cos(\phi_{ij})) \end{aligned} \tag{14}$$

Where $\phi_{ij} = \phi_i - \phi_j$

In most cases, these equations are numerically solved by iterative methods such as Gauss-Seider or Newton-Raphon.

For power systems operating near nominal conditions, the calculation of the nodal voltages is performed thanks to a linear approximation of the equations. Power flow linear equations are expressed by [22]:

$$P = -\mathbf{L}V \tag{15}$$

P is the vector of nodal active powers. V is the vector of nodal voltages and $\mathbf{L}$ is the DC bus admittance matrix. The complete derivation of this equation and the definition of $\mathbf{L}$ are given in Appendix B.

$\mathbf{L}$ is similar to the Laplacian matrix of the graph describing the grid. It is a singular matrix and the computation of the voltages from the powers is not straightforward. An option is to use the eigenvalues and eigenvectors of $\mathbf{L}$ [39]. For a path graph of N nodes, the eigenvalues and eigenvectors are noted λ_k and Ψ_k for $k \in \{0, 1, ..., N-1\}$. Their expressions are [40]:

$$\begin{aligned} \lambda_k &= 1 - cos(\frac{\pi k}{N}) \\ \Psi_{k,i} &= cos(\frac{\pi k i}{N} - \frac{\pi k}{2N}) \text{ for } i \in \{1, 2, ..., N\} \end{aligned} \tag{16}$$

$\Psi_{k,i}$ is the i-th entry of the eigenvector Ψ_k.

The nodal powers are expressed in the eigenbasis by:

$$P_i = \sum_{k=0}^{N-1} p_k \Psi_{k,i} \tag{17}$$

The derivation of the nodal voltages is straightforward and yields [41]:

$$V_i = \sum_{k=0}^{N-1} \frac{p_k}{\lambda_k} \Psi_{k,i} \tag{18}$$

From equations (3) and (4), the q-th correlation measure of the node voltages is defined by taking $\omega_{v,i} = V_i$ and it comes:

$$\langle \mu \rangle_q = \left\{ \frac{1}{N} \sum_{i \in \mathcal{N}} V_i \left[\frac{1}{N-1} \sum_{j \in \mathcal{N} \neq i} V_j \Theta(r - d_{i,j}) \right]^{q-1} \right\}^{\frac{1}{q-1}} \tag{19}$$

Using the spectral decomposition of the nodal voltages and the analytic expression of the eigenvalues and eigenvectors of a path graph, the q-th measure is calculated and results in a unit value for all the generalized dimensions as shown in Appendix B. This means that despite the inhomogeneous distribution of load powers along the line, the distribution of voltages is more homogeneous and scales linearly.

Using the implementation introduced in Appendix C, the multifractal spectra of the nodal powers and voltages are calculated numerically and compared with their theoretical expressions in figure 1. As expected, they are closed. Inaccuracies are caused by several factors. At small r, the statistics are generally too poor to be considered and when the maximal radius of the network is reached, the correlation measure saturates to 1. The range of observation is therefore limited and yields approximate values of scaling exponents. Another factor is related to the lacunar structure of the measure when high negative orders are considered. In [26], the lacunarities are cited as sources of errors for the estimation of the fractal dimensions because they cause intrinsic oscillations of the correlation integral. This explains why the accuracy drops more towards the right-hand side of the power spectrum where the correlation integral is dominated by the inverse of the lowest values of measures concentrated on very few nodes. This is less visible on voltage spectrum because the voltage values are more homogeneous.

4. Investigation of realistic test cases

Real distribution networks are more complex than path graphs. They are tree graphs and their line impedances are not identical. Three realistic medium voltage networks are investigated. The 69-bus case is derived from a part of PG&E distribution system used for delivering power to Northern and Central California [23]. The 85-bus test network is a rural distribution feeder [24]. The 141-bus network is a part of the distribution system of the metropolitan area of Caracas-Venezuela [25]. Their base values are shown in table 1. Their diagram and voltage profile are shown in figure 2. Some power flow results are given in table 2. The voltage values slightly decrease along the binomial network because of the voltage drops caused by the power flows in the branches. The voltage drops are larger for the realistic test cases than the binomial network. The main reasons are the differences in network geometries, line impedances and nodal distributions of loads active powers. But there is no obvious link between the shape of the networks and their voltages as shown in figure 2. Networks

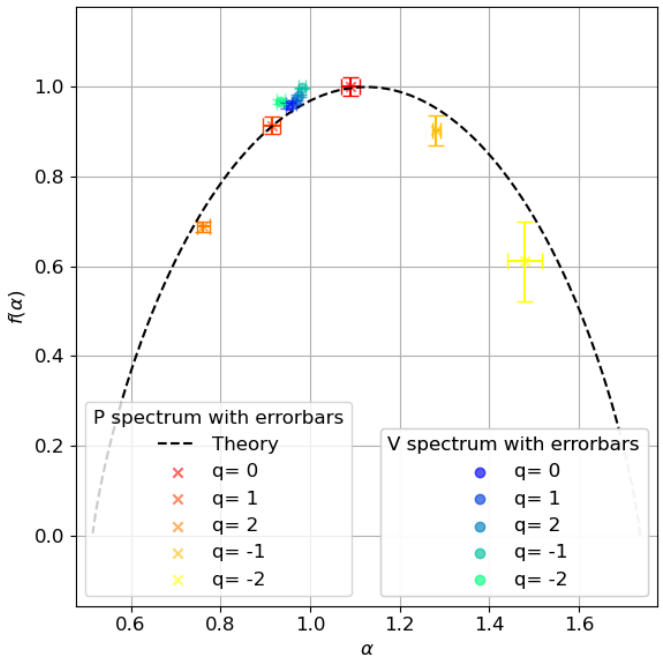

Figure 1: Multifractal spectra of the binomial network ($p_{binomial} = 0.7$ - $n = 7$)- The theoretical spectrum of the nodal powers is calculated by equations (8) and (9). The theoretical spectrum of the voltages is reduced to the $(1, 1)$ point. The practical determination of the spectra from the multifractal measures is done using equations (A.9) and (A.10). For the power spectrum, $\omega_{v,i} = P_i$. $\omega_{v,i} = V_i$ for the voltage spectrum. Error bars delimit the 95% confidence interval of the $f(\alpha)$ values identified by linear regression of the correlation measures.

electrical data are also compared in figure 3. Load power values are of the same order even if realistic values show more variations than the binomial network due to the connection of few industrial loads to the network. The 69 and 85-bus networks are more impedant than the binomial and the 141-bus case, meaning that the median value of their impedances are higher. In addition, these values are more widely distributed. The median values of X/R ratio between reactance X and resistance R of every lines are between 0.5 and 1 which are reasonable values for distribution power grids. From power flow results shown in table 2, the 85-bus network appears to be the worst case with the lowest minimal voltage value and the highest amount of losses despite of a low average nodal power. Again, there is no clear link between the network data and the power flow results.

Another view on the power flow results is offered by the multifractal spectra as shown in figure 4. Some metrics to characterize the spectra are defined. $f(\alpha_0)$ defines the maximum of the spectrum and is equal to the fractal dimension D_0 of the support. w_s is the width of the spectrum defined by $w_s = \alpha_{-2} - \alpha_2$.

Table 1: Test cases base values - In the per unit (p.u.) system, the system quantites are normalized and expressed as a fraction of a defined base value [22]. The base power S_b is chosen as the value of the apparent power of the substation that feeds the network. The base voltage V_b is chosen as the nominal rated voltage of the system. The base impedance is defined by $Z_b = \frac{V_b^2}{S_b}$. For the binomial network, $p = 0.7$ and $n = 7$.

	Binomial case	case 69	case 85	case 141
Number of nodes	129	69	85	141
Base voltage V_b (kV)	1	0.91	0.87	0.93
Base power S_b (MVA)	10	10	1	10
Base impedance Z_b (Ω)	10	10	1	10

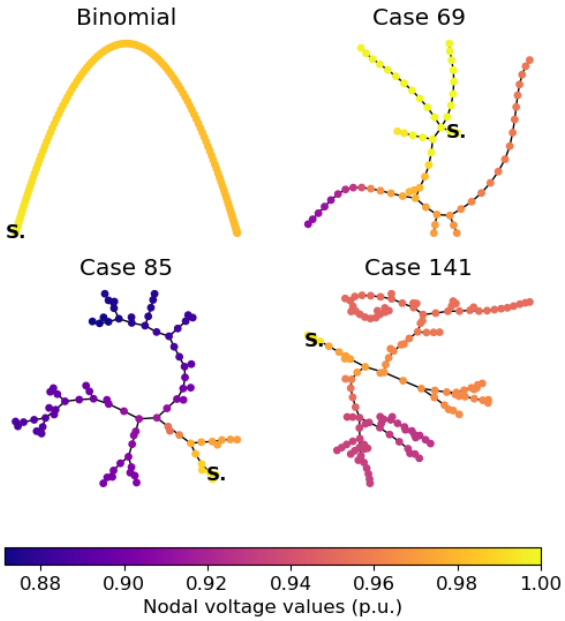

Figure 2: Nodal voltage magnitudes $|V_i|$ in per unit value (p.u.) of the test cases - The values are computed from power flow equations (14). They are normalized by the base voltage value V_b of each network. The source nodes are noted **S.**

a_s quantifies the skewness. It is given by $a_s = f(\alpha_{-2}) - f(\alpha_2)$. d_s gives the depth of the spectrum defined by $d_s = \frac{f(\alpha_{-2})+f(\alpha_2)}{2} - f(\alpha_0)$. Their values are given in table 3 together with some graph metrics. The networks lying down a 2-dimension support, their fractal dimension D_0 is between 1 and 2. The reference binomial network has a unit dimension and is monofractal (spectral width, depth and asymmetry are almost 0). The fractal dimensions of the realistic cases are higher than 1. This is a consequence of their ramifications.

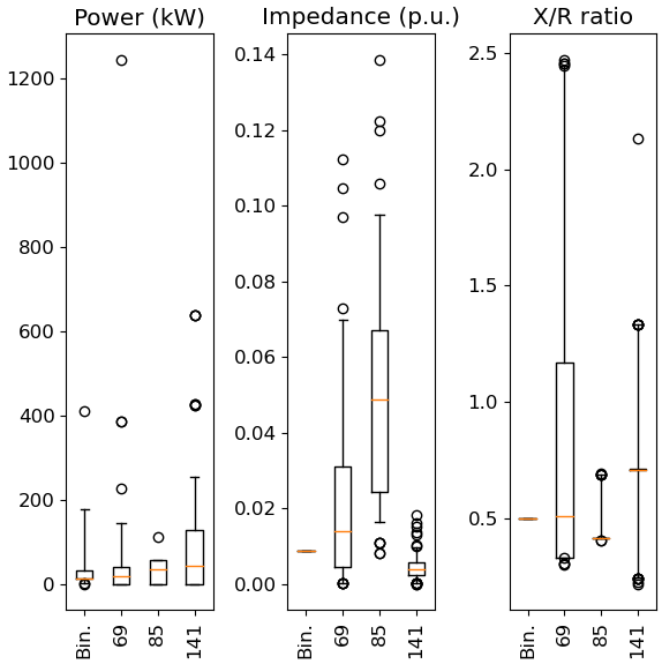

Figure 3: Comparison of electrical data of the test cases- Power panel gives the box plot of nodal active power data. Impedance panel gives $Z = \sqrt{R^2 + X^2}$ with R and X the line resistance and reactance respectively. Impedance value is normalized by the network's base impedance value Z_b. Boxes are delimited by the first and third quartiles. The median is shown by an horizontal line in the boxes. Whiskers extend from the 5th to 95th percentile and fliers points are located outside the whiskers. For the binomial network, $p_{binomial} = 0.7$ and $n = 7$.

The 69 and 85-bus networks show a wide spectral distribution. This may be caused by the dispersed distribution of their impedance values as shown in figure 3. The spectra of cases 69 and 141 are almost symmetric. The case 85 is right-skewed ($a_s < 0$) suggesting that the highest voltages are lying on a support with a dimension higher than the lowest values. The average node degree is near 2 which is an expected value for radial distribution networks [42]. The average node eccentricity gives an idea of the radius of the networks. Their graph density is near 0 meaning that they are very sparse.

While the classical graph metrics tend to stress the linear structure of the networks (nodes degree near 2, sparse networks, radius that are roughly increasing with the number of nodes), the multifractal characterization give a completely different view. But, to this point of the study, it fails to capture in a simple manner how structural parameters influence the voltage distributions. In particular, there is no obvious relation between power flow values, graph metrics and multifractal values.

Table 2: Power flow results - Min V is the per unit value of the minimal nodal voltage normalized by the network's base voltage V_b. Losses is the sum of the active losses in power lines normalized by the total load power. For the binomial network, $p = 0.7$ and $n = 7$.

	Binom.	69	85	141
Total load power (MW)	5	3.8	2.6	11.9
Min V (p.u.)	0.98	0.91	0.87	0.93
Losses (p.u.)	0.04	0.06	0.12	0.05
Average nodal power (MW)	0.039	0.055	0.03	0.084

Table 3: Network metrics - D_0, w_s, a_s and d_s are multifractal metrics. Other variables are graph metrics. The average degree is the average number of branches per node. The node eccentricity is defined as the maximum distance from one node to all others. The density is the ratio of the number of graph branches over the maximum possible number. For the binomial network, $p = 0.7$ and $n = 7$.

	Binomial case	Case 69	Case 85	Case 141
Fractal dimension D_0	$\approxeq 1$	1.27	1.68	1.26
Spectral width w_s	$\approxeq 0$	2.33	1.04	0.44
Spectral asymmetry a_s	$\approxeq 0$	-0.04	-0.28	-0.08
Spectral depth d_s	$\approxeq 0$	-0.73	-0.43	-0.21
Average node degree	1.98	1.97	1.98	1.99
Average node eccentricity	96	25.9	20.7	32.8
Graph density	0.016	0.029	0.024	0.014

5. Diffusion-limited aggregation grid expansion

To further determine the links between the structure of the networks and their steady-state values, a set of synthetic networks expanded by Diffusion-Limited Aggregation (DLA) is investigated. Hence, the objective is to determine how the parameters that control the DLA process and therefore the network structure determine the multifractal spectrum and the electrical properties.

Diffusion-Limited Aggregation is a process where diffusing particles aggregate to a cluster [16]. In 2-dimension, a seed is first placed on the space. Then a particle is placed on a random position and moves randomly until it aggregates to the seed. The process is then repeated with a new particle until it aggregates to the seed or the previous particle, and so on. It results from this process a random tree structure that has been widely used as a model for studying mechanisms of electrodeposition, dielectric breakdown, etc. In [43], a DLA growth process is conducted on a r-ary tree meaning that the DLA tree structure is constrained to be of r-ary type. In addition, the attachment probability p of the diffusing particle to a node located at the distance d to the root is such that:

$$p_{DLA} \sim (\alpha_{DLA})^d \tag{20}$$

This enables to control the shape of the tree. If the probability decreases with the distance ($\alpha_{DLA} > 1$), the height of the tree is logaritmically varying with the number of generations whereas it increases linearly when the probability

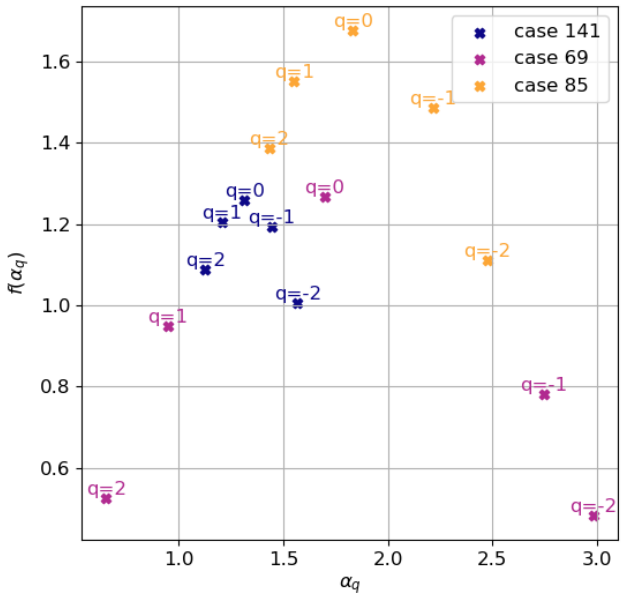

Figure 4: Singularity spectrum of the nodal voltages for the realistic test cases - The multifractal spectrum of the nodal voltages is computed by equations (A.9) and (A.10) for q between -2 and 2.

increases with the distance ($\alpha_{DLA} < 1$). In other words, the growth is more likely near the root or at the tips of the tree, resulting in different forms of the tree. The same method is used to synthesize the distribution grids.

To perform power flow calculations, some loads are distributed over the nodes. Following the toy network logic, their power values are randomly created by a binomial multiplicative cascade (see equation 6). This enables to control the distribution of the loads values. The nodes being numbered from the root, the binomial probability p_{bin} determines if loads are concentrated around the root node of the network or more likely connected at the termination nodes. The rank n of the cascade is such that $2^n + 1$ is the closest as possible of the actual number of nodes of the synthesized network.

The line reactance and resistance values are log-normally distributed. The log-normal distribution is chosen because of its asymmetry with a small proportion of high values. The mean of the line resistances values is $\frac{1}{2^n}$ and the X/R ratio is equal to 0.5 to be consistent with the values observed for the realistic networks in figure 3. The dispersion of the line values is controlled by the standard deviation σ.

To study the links between the structure, the steady-state values and the multifractal spectrum, a population of 2500 networks with 65 nodes is synthe-

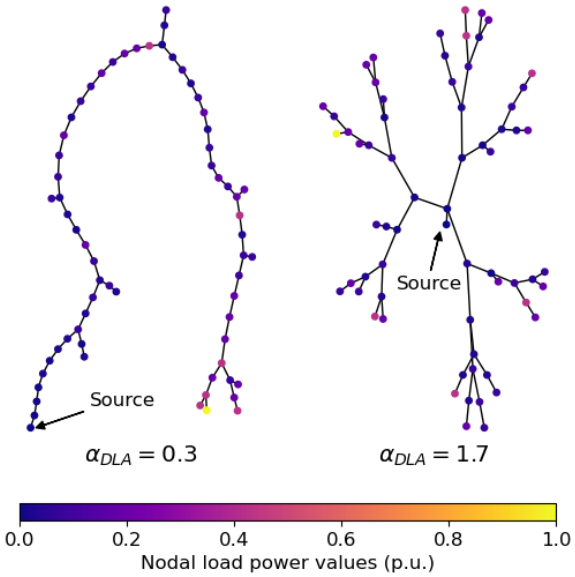

Figure 5: Example of networks given by a DLA-inspired growth method - The number of nodes is 65. The binomial probability is $p_{binomial} = 0.3$. Two extreme values of the growing parameter α_{DLA} are shown. On the left panel, the network is almost a path graph with very few bifurcations whereas on the right panel, the network is very ramified. In both cases, the loads are more concentrated at the end nodes of the network.

sized following our DLA approach. The networks are grown such that the nodes degree does not exceed 3 because the average degree is around 2 for realistic grids as previously seen in table 3. Two examples of synthesized structures are shown in figure 5. To be compared with realistic data, the sum of the load power values given by the multiplicative cascade has been normalized to be equal to the sum of the load power values of the 69-bus test case. The base power is also the same as the 69-bus one.

For every network, the observed variables are the total losses, the minimal node voltage, the fractal dimension D_0, the spectral width w_s, depth d_s and asymmetry a_s.

A Principal Component Analysis (PCA) is used to reduce the dimensionality of the synthesized multivariate data set and get a better interpretation of the variance. A first step in PCA is to calculate the percentage of variance explained by the components. This shows that two dimensions are enough to explain 90 % of the data variations. With three dimensions, almost 100 % is explained. To better understand the meaning of the PCA components, figure 6 gives the correlation values of the variables with the three first components.

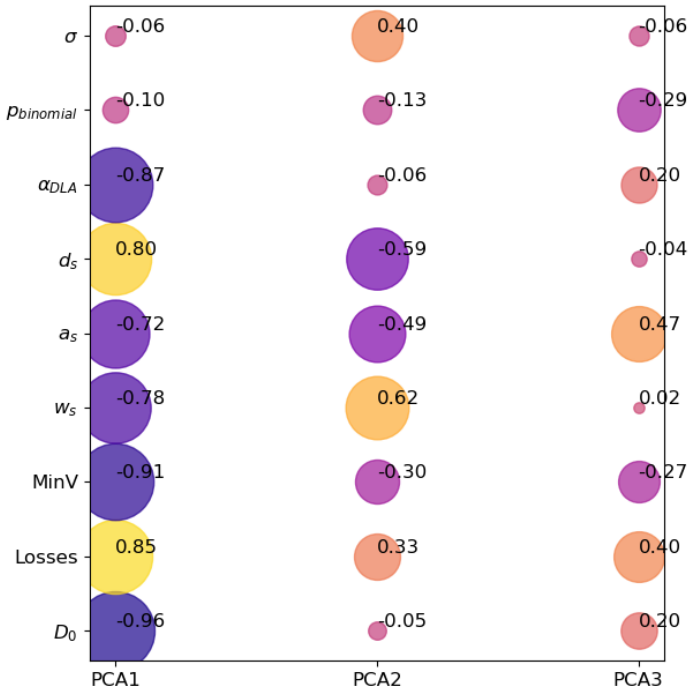

Figure 6: Correlation of the variables with the three first PCA components - The size of the circles is related to the absolute value of correlation. Their color is associated to the signed values.

α_{DLA}, multifractal metrics, eccentricity and power flow values have strong correlations with the first principal component. The explained variance by the first component being near 71%, the variations of the network performances and multifractal spectrum are predominantly determined by the growing parameter α_{DLA}. Note that the width and depth of the spectrum are very correlated. A wide spectrum shall therefore be deep.

The spectral depth, width and asymmetry are also correlated with the second axis as is the standard deviation of the impedance values σ. Their variations are thus influenced by the dispersion of the impedance values around their mean. The impact on the total losses and minimal voltage is found but limited. According to the explained variance, near 20% of the variations of the network's variables are driven by this second component.

The third component is the only one with a meaningful correlation with the binomial probability $p_{binomial}$. The asymmetry a_s is also correlated with this axis. So, the more the loads are located around the end nodes of the network giving more losses and voltage drops, the more left-skewed is the spectrum ($a_s > 0$). But this is only a correction of the influence of α_{DLA} which determines mostly the shape of the spectrum. Only 8% of the variations of the networks' variables are explained by this component.

The projections of the data onto the spaces constituted by the three first components are shown in figures 7 and 8. The biplots display at the same time the component scores (the position of each sample in the 2D-space) and the variable loadings (how variables correlate with components). Two nearby points represent two similar networks. The distribution of the points along with the first axis clearly shows that the networks grown with a small α_{DLA} are more elongated, have more losses and smaller voltage values. On the other hand, the networks grown with a large value of α_{DLA} result in fingered smaller networks, lesser losses and higher voltage values. Looking at variations along the second and third axis in figure 8, some previous tendencies may be reinforced by the dispersion of the line impedances values measured by σ. A high dispersion tends to give networks with more losses and voltage drops and a larger, deeper, more right-skewed network. A distribution of the loads towards the terminations of the network may explain an increase of the voltage drops, losses and left-skewness of the spectrum.

The three realistic cases are reported on both biplots. They are close to networks with a small growing parameter, indicating a linear structure. The cases 69 and 85 are noticeably located in the upper part of the second axis because of the large dispersion of their impedances values. The case 141 is a rather big network and its loads are more concentrated around the source as shown by its location in the lower part of the third axis.

6. Discussion and conclusion

Distribution networks are operated radially in normal conditions to supply power to all the loads. Radial topologies are optimal because they minimize the lenght of feeders and they require simple coordination scheme of protection devices. It can be noticed that they lack of redundant paths and normally open switches are added at the termination of the feeders so that he network can then be reconfigured by closing switches when a fault appears in the system and continue to deliver power to all the loads in the system [44, 45]. Spatial constraints are enforced on the position of the feeders when the distribution networks are planned [8, 46]. Feeders should follow the roads map. This prevents unrealistic design with feeders passing across or below the buildings. This gives very linear systems in rural area and the networks are more ramified in urban area. So, there is a strong coupling between the roads and the structure of the network [47] and coupled modeling of power networks and transportation systems is an emerging field [48].

We have proposed in this a paper a simple way to model and synthetize radial distribution networks. The synthetic grids are realistic networks that can be used to study the topological properties, how they are the results of design choices and how they drive the electrical properties [49].

Our method combines a DLA method to describe the grid expansion and a binomial multiplicative cascade to model the loads. This combination results in a rich variety of distribution grids. For low values of α_{DLA}, linear rural networks can be shaped. More ramified networks, closer to urban systems, are

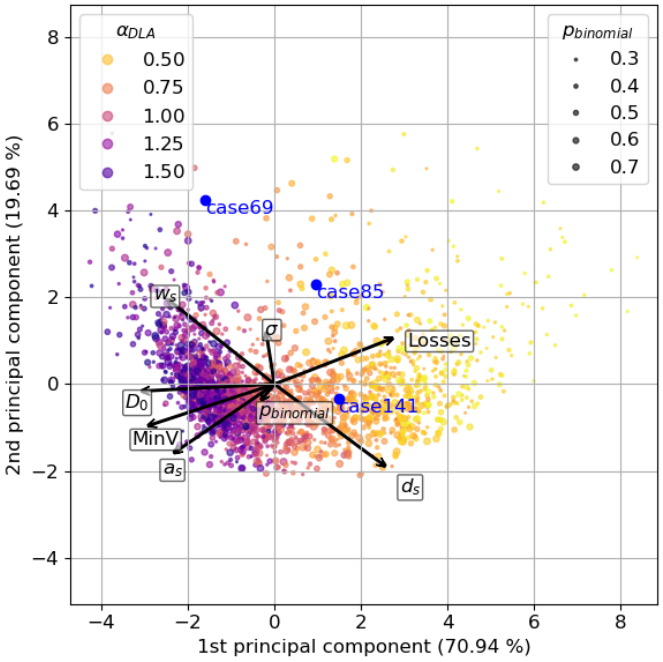

Figure 7: Biplot of 1^{st} and 2^{nd} principal components - The explained variance for each component is given between brackets. The expansion of the synthetized network is performed with a growing parameter α_{DLA} randomly chosen between 0.3 and 1.7. The load distribution is controlled by the binomial probability $p_{binomial}$ between 0.3 and 0.7. The standard deviation σ of the line parameters values is randomly chosen between 0.05 and 0.5.

also possible for intermediate values around the unit. For large values, it is even possible to shape cluster tree networks where clusters of nodes develop around the peripheral nodes. These networks could be suitable for community grids [50]. Community grids are consumer-centric microgrids where renewable energy sources and loads are located in the same area and connected together [51, 52]. They can be clusters of consumers in rural area where there is still no electrification or new home communities where many building are equipped with renewable energy sources and provide energy to the neighboring loads [53].

According to PCA's explained variance, the geometrical structure of the network is the main driver of the electrical properties and the values of impedances and loads have only a marginal impact on the network's voltage profile and total losses. Indeed, the loadings values on the second and third axis are smaller, meaning lesser variations of the variables with the corresponding components. Therefore, for power engineers and planners, a particular attention shall be first paid to the shape of the network in order to avoid violations of the normative voltage constraints and unexpected losses [54]. And corrective actions provided

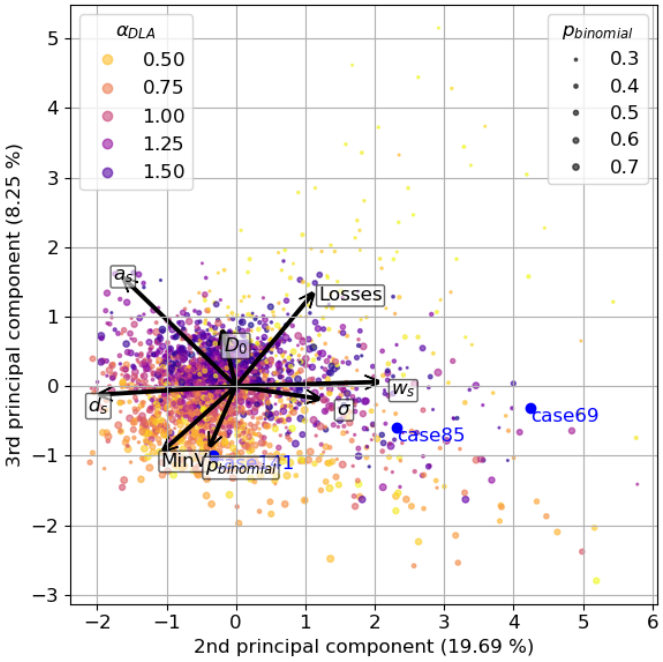

Figure 8: Biplot of 2^{nd} and 3^{rd} principal components

by variation of nodal powers (loads management or control of dispersed sources) will only have a marginal effect [9].

It has also been shown that distribution electrical networks are sparse tree-like networks with some self-similar branching that fall under the scope of multifractal studies. Multifractality is a way to classify power grids. It gives a set of parameters that can be used to perform clustering of networks as in [55].

To summarize, the fractal dimension gives an idea of the morphology of the network (with values between 1 and 2). Fractal dimensions were already used as a topological indicator [42]. They were compared with real data collected in China and other indicators such as node degree, network length, branching rate. But their values were not able to give a correct discrimination of topological properties of urban and suburban networks. To further investigate the fractal nature of distribution grids, an analogy was also done with a dielectric breakdown model in [56]. This is a mathematical model associated with the physical process of dielectric breakdown. It is closed to the diffusion-limited aggregation approach. This model was used to generate fractal electricity networks. Contrary to our approach, the load generation scheme was very basic, the same value being chosen for every loaded buses. The performances of the fractal networks were compared with real networks and confirm the fractal nature of real power distribution networks. No conclusion was drawn on the correlation between the

fractal dimension and the electrical properties of the synthetic networks.

For networks with nearby shapes and undiscriminating values of fractal dimension, the width of the multifractal spectrum may give an additional indication of the dispersion of the impedance values around their mean and the spectral asymmetry is a metric of the loads distribution for very similar networks. The multifractal variables are also correlated with the network eccentricity, losses and minimal voltages. The multifractal spectrum therefore gives a way of finely grading the networks by linking together their structure and electrical properties.

From this multifractal perspective, the best networks should have high fractal dimensions and low spectral asymmetry, depth and width, meaning ramified and compact network with a concentration of the high loads around the source node and homogeneous values of impedances. Some good candidates to investigate could be monofractal trees. Fractal patterns were already assessed for control architecture of power systems [57, 58]. Their introduction was motivated by the hierarchical structure of power systems from High Voltage to Low Voltage levels, the agile operation and easy reconfiguration or separation of the grid parts offered by the fractal geometry. In this approach, the control architecture is recursively built, every control level being self-similar. Only the parameters change depending on the voltage level that is controlled. This facilitates for the power engineers the description and the design of the power system.

Beyond control architecture, we propose that the power grid itself be fractal. This would be consistent with some previously published results on the interests of fractality for shaping cities [59]. Using fractal geometry turned out to be a promising approach for designing sustainable cities. It allows the development of green corridors penetrating urban areas and scaling down from large-scale green areas down to smaller ones. This helps saving biodiversity, providing accessibility to leisure areas and improving local climate by avoiding heat islands. At the same time, the fractal logic is used to plan a hierarchical system of urban centers of different size and functions. At local levels, shops for daily needs are present everywhere. Rarely frequented facilities are offered only at global levels. This provides proximity with shops and services proportional to their visit rate. Trip lengths and thus energy consumption and pollution are then reduced. Because roads map and distribution power grids are closely related, the fractal geometry is also used to design the electrical network with the same advantages of hierarchization and subsidiarity of power delivery. The distribution grid presents autonomous local levels where the loads are balanced by the production of renewable energy resources. They will however be linked hierarchically to higher levels to prevent any failure or large disturbance. So, fractal structures appears as optimal solutions for providing services over a wide range of scales at the lowest cost. The same observation was made in natural systems, e.g. the transportation network of nutrients in leaves or the river basins [60].

To conclude, even if this is still a long-term perspective, a plausible way to think the future of electrical energy grids is fractal and despite their apparent complexity, fractal geometry might be a right answer for energy networks.

Appendix A. Multifractal measures for power grids

To define the multifractal measures, an underlying graph G of a power grid is defined as $G = (\mathcal{N}, E, \omega_E)$ where $\mathcal{N}$ is the vertex set of size N, E is the edge set of size M along with the functions $\omega_v : \mathcal{N} \to \mathbb{R}$ and $\omega_e : E \to \mathbb{R}^+$ for the node and edge weights. The vertices are the grid nodes and the edges are the power lines. The node weights are equal to the nodal values (being voltage magnitude or power) normalized by the sum of all nodal values of the network. These values are the results of the solving of the power flow equations (14). The edge weights are the line impedances values.

The measure μ_i is defined by the sum of the values $\omega_{v,j}$ of the nodes j located within a cluster of radius r centered at the node i (see equation 4). The correlation integral is then given by:

$$\begin{aligned}\langle \mu \rangle =& \frac{1}{N} \sum_{i \in \mathcal{N}} \omega_{v,i} \mu_i(r) \\ =& \frac{1}{N} \sum_{i \in \mathcal{N}} \omega_{v,i} \frac{1}{N-1} \sum_{j \in \mathcal{N} \neq i} \omega_{v,j} \Theta(r - d_{i,j})\end{aligned} \tag{A.1}$$

The number of nodes of power grids being small, every nodes are taken as center. If this is too costful, it is obviously possible to limit the measure to a set of points randomly chosen in the network.

The q-th measure is defined for any $q \in \mathbb{N}^* - \{1\}$ by:

$$\langle \mu \rangle_q = \left\{ \frac{1}{N} \sum_{i \in \mathcal{N}} \omega_{v,i} \left[\frac{1}{N-1} \sum_{j \in \mathcal{N} \neq i} \omega_{v,j} \Theta(r - d_{i,j}) \right]^{q-1} \right\}^{\frac{1}{q-1}} \tag{A.2}$$

For $q = 1$, it is given by:

$$\langle \mu \rangle_1 = \lim_{q \to 1} \langle \mu_q \rangle = \exp \left[\sum_{i \in \mathcal{N}} \omega_{v,i} \ln(\mu_i(r)) \right] \tag{A.3}$$

Let us define:

$$\tau(q) = (q-1) D_q = \lim_{r \to 0} \frac{\ln \langle \mu^b \rangle_q(r)}{\ln(r)} \tag{A.4}$$

The Legendre transformation of (q, τ) is (α, f) such that:

$$\tau(q) = -f(\alpha(q)) + q\alpha(q) \tag{A.5}$$

$$q = \left. \frac{df(\alpha)}{d\alpha} \right|_{\alpha = \alpha(q)} \tag{A.6}$$

$$\alpha(q) = \frac{d\tau(q)}{dq} \tag{A.7}$$

Instead of using q and $\tau(q)$, the practical determination of the spectrum from the multifractal measures uses the equations A.5 and A.7 [37]. If we define:

$$\nu_i(q,r) = N \frac{[\mu_i(r)]^{q-1}}{\sum_{j\in\mathcal{N}} \omega_{v,j} [\mu_j(r)]^{q-1}} \tag{A.8}$$

Then:

$$\alpha(q) = \lim_{r\to 0} \frac{1}{\ln(r)} \frac{1}{N} \sum_{i\in\mathcal{N}} \omega_{v,i} \nu_i(q,r) \ln(\mu_i(r)) \tag{A.9}$$

And:

$$f(\alpha(q)) = \lim_{r\to 0} \frac{1}{\ln(r)} \frac{1}{N} \sum_{i\in\mathcal{N}} \omega_{v,i} \nu_i(q,r) \ln\left(\nu_i(q,r)\mu_i(r)\right) \tag{A.10}$$

Appendix B. Theoretical voltage spectrum of the binomial network

For linear approximation of the power flow equations (14), we assume that the binomial network is only resistive ($B_{ij} \approx 0$), the normalized voltage values are all near 1 ($|V_i| \approx 1$) and the phase differences between nodes are small ($\phi_{ij} \approx 0$). It means that the binomial network behaves as a DC resistive network.

Therefore, the only variables are the voltages and the active powers. They are linked by:

$$P_i = \sum_{j=1}^{N} B_{ij} V_j \tag{B.1}$$

Under a matrix form, this relation is written:

$$P = -\mathbf{L}V \tag{B.2}$$

$\mathbf{L}$ is the so-called DC bus admittance matrix.

The q-th correlation measure of the voltage distribution is given by equation (19). Assuming a large number of nodes, a continuous approximation of this measure is considered. It means that over the path length, being normalized to 1, the double discrete sum is approximated by a double integral. At every position $x \in [0,1]$ on the path, the voltage magnitude is noted V_x. Hence:

$$\langle\mu\rangle_q^{q-1} \sim \int_0^1 V_y \left[\int_0^1 V_x \Theta(r - |x-y|) dx\right]^{q-1} dy \tag{B.3}$$

Using equations (16) and (18), the double integral is written:

$$\langle\mu\rangle_q^{q-1} \sim \sum_{k'=0}^{N-1} \frac{p_{k'}}{\lambda_{k'}} \int_0^1 cos(\pi k' x - \frac{\pi k'}{2N}) \left[\sum_{k=0}^{N-1} \frac{p_k}{\lambda_k} I(r,y)\right]^{q-1} dy \tag{B.4}$$

With:

$$\begin{aligned} I(r,y) = &\int_0^y cos(\pi k x - \frac{\pi k}{2N})\Theta(r-y+x)dx \\ &+ \int_y^1 cos(\pi k x - \frac{\pi k}{2N})\Theta(r-x+y)dx \end{aligned} \tag{B.5}$$

$\Theta(z) = 1$ if $z > 0$. Thus $\Theta(r-y+x) = 1$ if $x > y-r$ and $\Theta(r-y+x) = 1$ if $x < y+r$. Otherwise, it is 0. This results in four cases as shown in table B.4.

Table B.4: Expressions of $I(r,y)$

case	y interval	$I(r,y)$
1	$y-r<0$ and $y+r<1$	$\int_0^y cos(\pi k x - \frac{\pi k}{2N})dx + \int_y^{y+r} cos(\pi k x - \frac{\pi k}{2N})dx$ $= \frac{1}{\pi k}\left[sin(\pi k(y+r) - \frac{\pi k}{2N}) + sin(\frac{\pi k}{2N})\right]$
2	$y-r<0$ and $y+r>1$	$\int_0^y cos(\pi k x - \frac{\pi k}{2N})dx + \int_y^1 cos(\pi k x - \frac{\pi k}{2N})dx$ $= \frac{1}{\pi k}\left[sin(\pi k - \frac{\pi k}{2N}) + sin(\frac{\pi k}{2N})\right]$
3	$y-r>0$ and $y+r<1$	$\int_{y-r}^y cos(\pi k x - \frac{\pi k}{2N})dx + \int_y^{y+r} cos(\pi k x - \frac{\pi k}{2N})dx$ $= \frac{1}{\pi k}\left[sin(\pi k(y+r) - \frac{\pi k}{2N}) - sin(\pi k(y-r) - \frac{\pi k}{2N})\right]$
4	$y-r>0$ and $y+r>1$	$\int_{y-r}^y cos(\pi k x - \frac{\pi k}{2N})dx + \int_y^1 cos(\pi k x - \frac{\pi k}{2N})dx$ $= \frac{1}{\pi k}\left[sin(\pi k - \frac{\pi k}{2N}) - sin(\pi k(y-r) - \frac{\pi k}{2N})\right]$

The following integral is then calculated:

$$J(r) = \int_0^1 cos(\pi k' y - \frac{\pi k'}{2N}) \left[\sum_{k=0}^{N-1} \frac{p_k}{\lambda_k} I(r,y)\right]^{q-1} dy \tag{B.6}$$

In this integral, the expression of $I(r,y)$ depends on the relative position of y, r and $1/2$. It is known from equation (5) that only the limit of the correlation integral when r tends to 0 matters. Hence, the calculation of $J(r)$ is reduced to case 3 in table B.4. In addition, r tending to zero, the sinus function may be

approximated by its argument. It results:

$$\langle\mu\rangle_q^{q-1} \sim r^{q-1} \sum_{k'=0}^{N-1} \frac{p_{k'}}{\lambda_{k'}} \int_0^1 cos(\pi k' y - \frac{\pi k'}{2N}) \left[\sum_{k=0}^{N-1} \frac{p_k}{\lambda_k} \frac{2}{\pi k} cos(\pi k y - \frac{\pi k}{2N}) \right]^{q-1} dy \tag{B.7}$$

Thus, in any case, $\langle\mu\rangle_q^{q-1}$ is proportional to r^{q-1}. So whatever is the distribution of the loads, the generalized dimensions defined by equation 5 are equal to $D_q = 1$ for any q.

Following Legendre transformation equations (A.5), (A.6) and (A.7), it comes:

$$\tau(q) = q - 1 \tag{B.8}$$

$$\alpha(q) = 1 \tag{B.9}$$

$$f(\alpha) = 1 \tag{B.10}$$

The theoretical spectrum of the voltages is reduced to a single point $(1, 1)$.

Appendix C. Implementation

The solving of power flow equations (14) is done using a *Python* package called *Pypower*.

A *Python* code has been developed to implement the correlation method for nodal weighted networks. A graph traversal procedure is used to calculate correlation measures. The correlation radius is calculated from inter-node distances that are taken equal to line impedance values. Depending on which values are measured, nodes weights are either taken equal to nodal powers or voltages. For computing the slopes of the log-log variations of the correlation measures, the linear regression package *Linregress* of *Python* is used.

The Diffusion-Limited-Aggregation process on a tree has also been implemented under *Python* and the *Scikit-Learn* machine learning library has been used for PCA analysis.

The realistic test case data are publicly available. They come from [23, 24, 25].

Competing Interests statement

The authors have declared no conflict of interest for this article.

Acknowledgment

This work benefited from the support of the project FRACTAL GRID ANR-15-CE05-007-01 led by the French National Research Agency (ANR).

References

[1] C. Arderne, C. Zorn, C. Nicolas, and E. E. Koks. Predictive mapping of the global power system using open data. *Scientific Data*, 7(1):19, December 2020.

[2] N Andreadou, M. G Flammini, Gianluca Fulli, M Masera, Giuseppe Prettico, S Vitiello, European Commission, and Joint Research Centre. *Distribution system operators observatory 2018: overview of the electricity distribution system in Europe.* 2019. OCLC: 1111251973.

[3] J. Lowitzsch, C. E. Hoicka, and F. J. van Tulder. Renewable energy communities under the 2019 European Clean Energy Package – Governance model for the energy clusters of the future? *Renewable and Sustainable Energy Reviews*, 122:109489, April 2020.

[4] Emil Hillberg, Antony Zegers, Barbara Herndler, Steven Wong, Jean Pompee, Jean-Yves Bourmaud, Sebastian Lehnhoff, Gianluigi Migliavacca, Kjetil Uhlen, Irina Oleinikova, Hjalmar Pihl, Markus Norström, Mattias Persson, Joni Rossi, and Giovanni Beccuti. Flexibility needs in the future power system. Technical report, March 2019.

[5] Adam Hirsch, Yael Parag, and Josep Guerrero. Microgrids: A review of technologies, key drivers, and outstanding issues. *Renewable and Sustainable Energy Reviews*, 90:402–411, July 2018.

[6] S. Ma, L. Su, Z. Wang, F. Qiu, and G. Guo. Resilience Enhancement of Distribution Grids Against Extreme Weather Events. *IEEE Transactions on Power Systems*, 33(5):4842–4853, September 2018.

[7] A. T. D. Perera, Silvia Coccolo, and Jean-Louis Scartezzini. The influence of urban form on the grid integration of renewable energy technologies and distributed energy systems. *Scientific Reports*, 9(1):17756, December 2019.

[8] J. Shu, L. Wu, Z. Li, M. Shahidehpour, L. Zhang, and B. Han. A New Method for Spatial Power Network Planning in Complicated Environments. *IEEE Transactions on Power Systems*, 27(1):381–389, February 2012.

[9] N. C. Koutsoukis, P. S. Georgilakis, and N. D. Hatziargyriou. Multistage Coordinated Planning of Active Distribution Networks. *IEEE Transactions on Power Systems*, 33(1):32–44, January 2018.

[10] V. Vahidinasab, M. Tabarzadi, H. Arasteh, M. I. Alizadeh, M. Mohammad Beigi, H. R. Sheikhzadeh, K. Mehran, and M. S. Sepasian. Overview of Electric Energy Distribution Networks Expansion Planning. *IEEE Access*, 8:34750–34769, 2020.

[11] Mark A. Bedau. Weak Emergence. *Noûs*, 31(s11):375–399, 1997.

[12] B. B. Mandelbrot. *The fractal geometry of nature*. W. H. Freeman and Comp., New York, 3 edition, 1983.

[13] G. Parisi and U. Frisch. On the singularity structure of fully developed turbulence. *Proceed. Turbulence and Predictability in Geophysical Fluid Dynamics and Climate Dynamics*, pages 84–88, 1985.

[14] P. Pavón-Domínguez, A.B. Ariza-Villaverde, A. Rincón-Casado, E. Gutiérrez de Ravé, and F.J. Jiménez-Hornero. Fractal and multifractal characterization of the scaling geometry of an urban bus-transport network. *Computers, Environment and Urban Systems*, 64:229–238, July 2017.

[15] Mahmoud Saeedimoghaddam and T. F. Stepinski. Multiplicative random cascade models of multifractal urban structures. *Physica A: Statistical Mechanics and its Applications*, 569:125767, May 2021.

[16] T. A. Witten and L. M. Sander. Diffusion-limited aggregation. *Physical Review B*, 27(9):5686–5697, May 1983.

[17] M Batty, P Longley, and S Fotheringham. Urban Growth and Form: Scaling, Fractal Geometry, and Diffusion-Limited Aggregation. *Environment and Planning A: Economy and Space*, 21(11):1447–1472, November 1989.

[18] L.S. Safavian, W. Kinsner, and H. Turanli. Classification of transients in power systems using multifractal analysis. In *Canadian Conference on Electrical and Computer Engineering 2004 (IEEE Cat. No.04CH37513)*, volume 3, pages 1445–1448 Vol.3, May 2004. ISSN: 0840-7789.

[19] Tejun Zhou, Jiazheng Lu, Bo Li, and Yanjun Tan. Fractal Analysis of Power Grid Faults and Cross Correlation for the Faults and Meteorological Factors. *IEEE Access*, 8:79935–79946, 2020.

[20] Joel D. Melo, Edgar M. Carreno, Antonio Padilha-Feltrin, and Carlos R. Minussi. Grid-based simulation method for spatial electric load forecasting using power-law distribution with fractal exponent. *International Transactions on Electrical Energy Systems*, 26(6):1339–1357, 2016.

[21] National Academies of Sciences, Engineering, and Medicine. *Analytic Research Foundations for the Next-Generation Electric Grid*. The National Academies Press, Washington, DC, 2016.

[22] Prabha S. Kundur. *Power System Stability And Control*. EPRI power system engineering series. McGraw-Hill, 1st edition, 1994.

[23] Mesut Baran and Felix F. Wu. Optimal sizing of capacitors placed on a radial distribution system. *IEEE Transactions on power Delivery*, 4(1):735–743, 1989.

[24] D. Das, D. P. Kothari, and A. Kalam. Simple and efficient method for load flow solution of radial distribution networks. *International Journal of Electrical Power & Energy Systems*, 17(5):335–346, October 1995.

[25] H. M. Khodr, F. G. Olsina, P. M. De Oliveira-De Jesus, and J. M. Yusta. Maximum savings approach for location and sizing of capacitors in distribution systems. *Electric Power Systems Research*, 78(7):1192–1203, July 2008.

[26] James Theiler. Estimating fractal dimension. *JOSA A*, 7(6):1055–1073, 1990.

[27] Peter Grassberger and Itamar Procaccia. Measuring the strangeness of strange attractors. *Physica D: Nonlinear Phenomena*, 9(1-2):189–208, 1983.

[28] Peter Grassberger and Itamar Procaccia. Characterization of Strange Attractors. *Physical Review Letters*, 50(5):346–349, January 1983.

[29] Peter Grassberger and Itamar Procaccia. Estimation of the Kolmogorov entropy from a chaotic signal. *Physical Review A*, 28(4):2591–2593, October 1983.

[30] H. G. E. Hentschel and Itamar Procaccia. The infinite number of generalized dimensions of fractals and strange attractors. *Physica D: Nonlinear Phenomena*, 8(3):435–444, 1983.

[31] K. Pawelzik and H. G. Schuster. Generalized dimensions and entropies from a measured time series. *Physical Review A*, 35(1):481–484, January 1987.

[32] Tamás Tél, Ágnes Fülöp, and Tamás Vicsek. Determination of fractal dimensions for geometrical multifractals. *Physica A: Statistical Mechanics and its Applications*, 159(2):155–166, 1989.

[33] Chaoming Song, Shlomo Havlin, and Hernán A. Makse. Self-similarity of complex networks. *Nature*, 433(7024):392–395, January 2005.

[34] Yu-Qin Song, Jin-Long Liu, Zu-Guo Yu, and Bao-Gen Li. Multifractal analysis of weighted networks by a modified sandbox algorithm. *Scientific Reports*, 5:17628, December 2015.

[35] H. S. Greenside, A. Wolf, J. Swift, and T. Pignataro. Impracticality of a box-counting algorithm for calculating the dimensionality of strange attractors. *Physical Review A*, 25(6):3453–3456, June 1982.

[36] Thomas C. Halsey, Mogens H. Jensen, Leo P. Kadanoff, Itamar Procaccia, and Boris I. Shraiman. Fractal measures and their singularities: the characterization of strange sets. *Physical Review A*, 33(2):1141, 1986.

[37] Ashvin Chhabra and Roderick V. Jensen. Direct determination of the singularity spectrum. *Physical Review Letters*, 62(12):1327, 1989.

[38] Jens Feder. *Fractals*. Number Physics of Solids and Liquids. Springer US, Boston, MA, 1st edition, 1988.

[39] N. Retière, D. T. Ha, and J. Caputo. Spectral Graph Analysis of the Geometry of Power Flows in Transmission Networks. *IEEE Systems Journal*, pages 1–12, 2019.

[40] Fan R. K. Chung. *Spectral Graph Theory*. American Mathematical Society, Providence, RI, 1997.

[41] J G Caputo, A Knippel, and N Retiere. Spectral analysis of load flow equations for transmission networks. *Engineering Research Express*, 1(2):025007, October 2019.

[42] Sathsara Abeysinghe, Jianzhong Wu, Mahesh Sooriyabandara, Muditha Abeysekera, Tao Xu, and Chengshan Wang. Topological properties of medium voltage electricity distribution networks. *Applied Energy*, 210:1101–1112, January 2018.

[43] Martin T. Barlow, Robin Pemantle, and Edwin A. Perkins. Diffusion-limited aggregation on a tree. *Probability Theory and Related Fields*, 107(1):1–60, January 1997.

[44] Y-. Y Hsu and Y. Jwo-Hwu. Planning of distribution substations, feeders and sectionalizing switches using heuristic algorithms. *International Journal of Electrical Power & Energy Systems*, 18(5):315–322, June 1996.

[45] Saheli Ray, Aniruddha Bhattacharya, and Subhadeep Bhattacharjee. Optimal placement of switches in a radial distribution network for reliability improvement. *International Journal of Electrical Power & Energy Systems*, 76:53–68, March 2016.

[46] James R. E. Fletcher, Tyrone Fernando, Herbert Ho-Ching Iu, Mark Reynolds, and Shervin Fani. Spatial Optimization for the Planning of Sparse Power Distribution Networks. *IEEE Transactions on Power Systems*, 33(6):6686–6695, November 2018.

[47] Yousra Sidqi, Isabelle Thomas, Pierre Frankhauser, and Nicolas Retière. Comparing fractal indices of electric networks to roads and buildings: The case of Grenoble (France). *Physica A: Statistical Mechanics and its Applications*, 531:121774, October 2019.

[48] Yingyun Sun, Pengfei Zhao, Liwei Wang, and Sarmad Majeed Malik. Spatial and temporal modelling of coupled power and transportation systems: A comprehensive review. *Energy Conversion and Economics*, 2(2):55–66, 2021.

[49] Giuliano Andrea Pagani and Marco Aiello, Rijksuniversiteit Groningen. *From the grid to the smart grid, topologically*. PhD thesis, Rijksuniversiteit Groningen, Groningen, 2014. OCLC: 870964717.

[50] F. Bandeiras, E. Pinheiro, M. Gomes, P. Coelho, and J. Fernandes. Review of the cooperation and operation of microgrid clusters. *Renewable and Sustainable Energy Reviews*, 133:110311, November 2020.

[51] Rohit Trivedi, Sandipan Patra, Yousra Sidqi, Benjamin Bowler, Fiona Zimmermann, Geert Deconinck, Antonios Papaemmanouil, and Shafi Khadem. Community-Based Microgrids: Literature Review and Pathways to Decarbonise the Local Electricity Network. *Energies*, 15(3):918, January 2022.

[52] Paolo Tenti and Tommaso Caldognetto. On Microgrid Evolution to Local Area Energy Network (E-LAN). *IEEE Transactions on Smart Grid*, 10(2):1567–1576, March 2019.

[53] Pedro Ciller, Douglas Ellman, Claudio Vergara, Andres Gonzalez-Garcia, Stephen J. Lee, Cailinn Drouin, Matthew Brusnahan, Yael Borofsky, Carlos Mateo, Reja Amatya, Rafael Palacios, Robert Stoner, Fernando de Cuadra, and Ignacio Perez-Arriaga. Optimal Electrification Planning Incorporating On- and Off-Grid Technologies: The Reference Electrification Model (REM). *Proceedings of the IEEE*, 107(9):1872–1905, September 2019.

[54] D. Ciechanowicz, D. Pelzer, B. Bartenschlager, and A. Knoll. A Modular Power System Planning and Power Flow Simulation Framework for Generating and Evaluating Power Network Models. *IEEE Transactions on Power Systems*, 32(3):2214–2224, May 2017.

[55] Tobias Rösch and Peter Treffinger. Cluster Analysis of Distribution Grids in Baden-Württemberg. *Energies*, 12(20):4016, October 2019.

[56] F. Barakou, D. Koukoula, N. Hatziargyriou, and A. Dimeas. Fractal geometry for distribution grid topologies. In *2015 IEEE Eindhoven PowerTech*, pages 1–6, Eindhoven, Netherlands, June 2015. IEEE.

[57] E. Ortjohann, P. Wirasanti, A. Schmelter, H. Saffour, M. Hoppe, and D. Morton. Cluster fractal model—A flexible network model for future power systems. In *Clean Electrical Power (ICCEP), 2013 International Conference on*, pages 293–297. IEEE, 2013.

[58] Albana Ilo. Design of the Smart Grid Architecture According to Fractal Principles and the Basics of Corresponding Market Structure. *Energies*, 12(21):4153, October 2019.

[59] Pierre Frankhauser. Fractalopolis—A Fractal Concept for the Sustainable Development of Metropolitean Areas. In Patricia Sajous and Cyrille Bertelle, editors, *Complex Systems, Smart Territories and Mobility*, Understanding Complex Systems, pages 15–50. Springer International Publishing, Cham, 2021.

[60] Jon D. Pelletier and Donald L. Turcotte. Shapes of river networks and leaves: are they statistically similar? *Philosophical Transactions of the Royal Society of London. Series B: Biological Sciences*, 355(1394):307–311, February 2000.

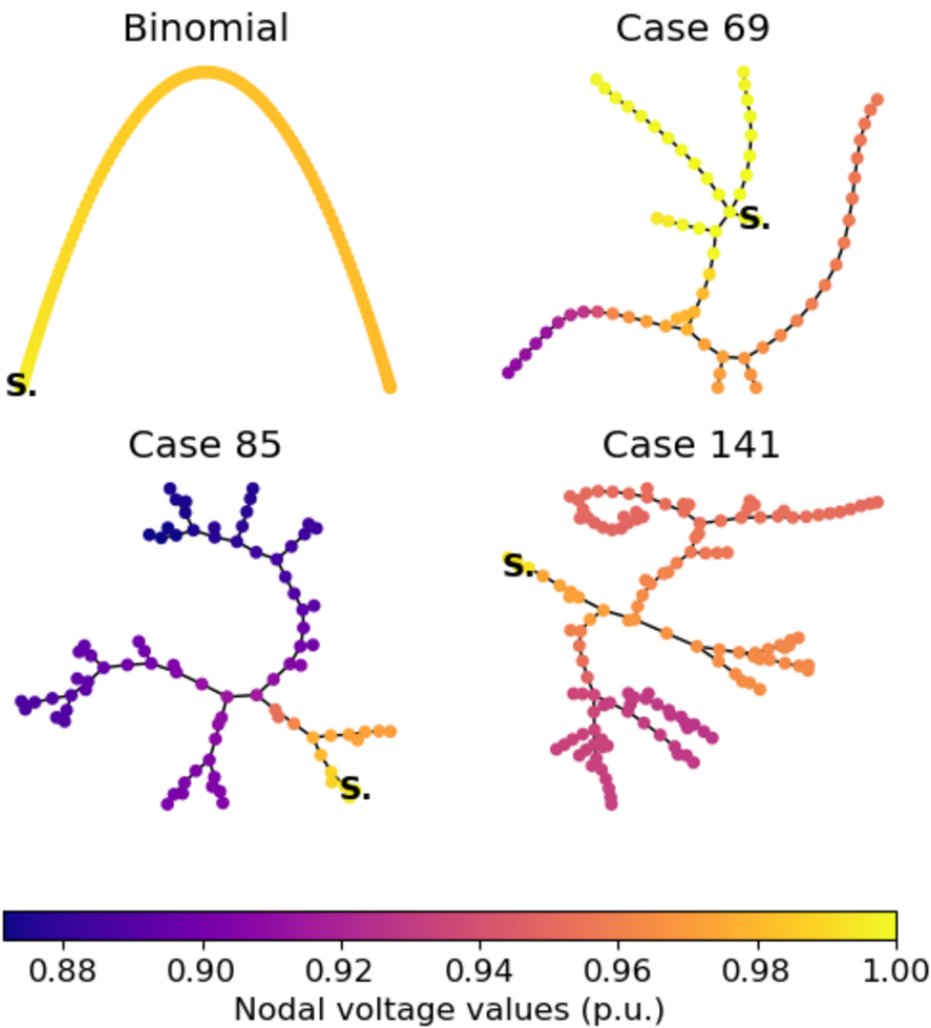
Binomial
Case 69
Case 85
Case 141
S.
S.
S.
S.
0.88
0.90
0.92
0.94
0.96
0.98
1.00
Nodal voltage values (p.u.)